

## Nucleosome-like Complex of the Histone from the Hyperthermophile *Methanopyrus Kandleri* (MkaH) with Linear DNA

<http://www.jbsdonline.com>

Nikolai A. Pavlov<sup>1,2,3</sup>  
Dmitry I. Cherny<sup>1,4,\*</sup>  
Thomas M. Jovin<sup>1</sup>  
Alexei I. Slesarev<sup>3,5</sup>

<sup>1</sup>Department of Molecular Biology  
Max Planck Institute for Biophysical  
Chemistry

Am Fassberg 11, D-37077  
Göttingen, Germany

<sup>2</sup>Belozersky Institute of Physico-  
Chemical Biology

Moscow State University  
119899 Moscow, Russia

<sup>3</sup>M. M. Shemyakin and Yu. A.  
Ovchinnikov Institute of Bioorganic  
Chemistry

Russian Academy of Sciences  
117871 Moscow, Russia

<sup>4</sup>Institute of Molecular Genetics  
Russian Academy of Sciences  
Kurchatov's Square  
Moscow, Russia

<sup>5</sup>Fidelity Systems, Inc.  
Gaithersburg, Maryland 20879, USA

### Abstract

The MkaH protein from the archaeon *Methanopyrus kandleri*, an unusual assembly of two histone-fold domains in a single polypeptide chain, demonstrates high structural similarity to eukaryal histones. We studied the DNA binding and self-association properties of MkaH by means of the electrophoretic mobility shift assay (EMSA), electron microscopy (EM), chemical cross-linking, and analytical gel filtration. EMSA showed an increased mobility of linear DNA complexed with MkaH protein with a maximum at a protein-DNA weight ratio ( $R_w$ ) of  $\approx 3$ ; the mobility decreased at higher protein concentration. EM of the complexes formed at  $R_w \leq 3$  revealed formation of isometric loops encompassing  $71 \pm 7$  bp of DNA duplex. At high values of  $R_w$  ( $\geq 9$ ) thickened compact nucleoprotein structures were observed; no individual loops were seen within the complexes. Gel filtration chromatography and chemical fixation indicated that in the absence of DNA the dominant form of the MkaH in solution, unlike other archaeal histones, is a stable dimer (pseudo-tetramer of the histone-fold domain) apparently resembling the eukaryal (H3-H4)<sub>2</sub> tetramer. Similarly, dimers are the dominant form of the protein interacting with DNA. The properties of MkaH supporting the assignment of its intermediate position between other archaeal and eukaryal histones are discussed.

Key words: histone/ nucleosome/ hyperthermophile/ *Methanopyrus kandleri*/ DNA wrapping

### Introduction

The hyperthermophilic methanogen *Methanopyrus kandleri* can grow at temperatures of up to 110° C and has an intracellular K<sub>3</sub> cyclic 2,3-diphosphoglycerate concentration of 1.1 M (1). *Methanopyrus kandleri* possesses a number of properties that make it unique amongst archaeal species, indicating a possible relation to the last common ancestor of Archaea and Eukarya. To our knowledge, *M. kandleri* is the only archaeon that contains a type IB topoisomerase, previously found in eukaryotes and poxviruses (2, 3). Based on the 16S RNA derived phylogenetic tree, the microorganism represents a very early branch-off within the archaeal kingdom Euryarchaeota, without bearing any close relationship to other methanogens (4). The ancestry of *M. kandleri* and its phylogenetic link to Eukarya is further supported by the properties of the histone protein identified in this organism (5).

In Eukarya, histones H3, H4, H2A, and H2B play a major role in DNA condensation. The nucleosome core particle, the primary package unit of eukaryal chromatin, contains two copies of each histone within a histone octamer; 145-147 bp-long DNA is wrapped around the octamer into 1.65 negative superhelical turns (6). The central part of the nucleosome is constituted by the tetramer of histones H3 and

\*Phone: +49 (0) 551 201 1383  
Fax: +49 (0) 551 201 1467  
Email: dcherny1@gwdg.de

**Abbreviations:** EMSA, electrophoretic mobility shift assay; EM, electron microscopy; K-Glu, potassium glutamate.

H4, which exists as a stable particle in the absence of DNA (7). It has been suggested that the tetrasome, a complex of the (H3-H4)<sub>2</sub> tetramer and DNA, is an important intermediate in nucleosome transactions (8, 9).

Nucleosome-mediated DNA compaction was interpreted as a distinctive feature of Eukarya before the discovery of histone homologues in Euryarchaeota (10). The structure of archaeal histones is closely related to that of the histone-fold domain, a conserved histone unit mediating octamer assembly and DNA binding (11). Archaeal histones were shown to form nucleosome-like particles, constituted by ~80 bp of DNA wrapped around the protein tetramer (12). Such a composition is reminiscent of the eukaryal tetrasome rather than the full-size nucleosome.

The MkaH histone isolated from *M. kandleri* has a very unusual structure, containing two histone-fold domains connected by a 13 amino acid loop in a single chain. Intriguingly, phylogenetic reconstruction analysis showed that its N-terminal domain is more closely related to eukaryal histones than to any other archaeal counterpart (5). From crystallographic analysis, the three-dimensional structure of the entire protein resembles eukaryal H3/H4 and H2A/H2B heterodimers, as well as archaeal homodimers HMfA<sub>2</sub> and HMfB<sub>2</sub> (13). In the crystal, two MkaH molecules are assembled into a dimer, which is structurally similar to the (H3-H4)<sub>2</sub> tetramer observed in the eukaryal nucleosome. In contrast, other previously characterized archaeal histones did not form such structures in the absence of DNA either in crystals or in solution.

In this study, we characterize the self-association and DNA-binding properties of the MkaH histone. We infer from the experimental data that in solution MkaH forms a stable dimer similar to the eukaryal tetramer, whereas in the presence of DNA it constrains 71 +/- 7 bp of DNA duplex into small loops yielding a particle homologous to the eukaryal tetrasome.

### **Materials and Methods**

#### *Purification of the recombinant MkaH protein*

Bacterial cells BL21 (DE3) pLysS carrying the MkaH-expressing plasmid pET11 were grown at 37° C to A<sub>600</sub> = 0.5 and MkaH expression was induced by adding IPTG to a final concentration of 0.4 mM, followed by further growth at 37° C for 3 h. Cells were harvested and stored at -20° C overnight. Then the pellet was thawed at 37° C for 5 min, resuspended in buffer LT (1 M NaCl, 5% glycerol, 20 mM Tris-HCl, pH 8.0, 10 mM β-mercaptoethanol, 1 mM PMSF) and incubated at the same temperature for 5 min, sufficient for cell lysis. Following the centrifugation (20000×g, 10 min, 4° C), the cleared supernatant was incubated at 80° C for 10 min and centrifuged (20000×g, 10 min, 4° C) to remove non-thermostable proteins. The crude extract was diluted 4-fold and applied to a HiTrap heparin column (Bio-Rad). MkaH protein was eluted with a NaCl gradient (0.4 M – 1 M); the MkaH-containing fractions were collected and concentrated using Centricon-10 cartridges (Amicon) with reducing NaCl concentration to 250 mM. Under these conditions MkaH formed crystals, which were collected by centrifugation and dissolved either in buffer LT or LP (1 M NaCl, 5% glycerol, 10 mM Na-Hepes, pH 8.0, 10 mM β-mercaptoethanol, 1 mM PMSF).

#### *Electrophoretic Mobility Shift Assay (EMSA)*

To obtain MkaH-DNA complexes, 100 ng of *Bam*HI linearized pUC19 DNA was incubated with MkaH at various protein-DNA weight ratios in buffer A containing 1 M potassium glutamate (K-Glu), 20 mM Tris-HCl, pH 8.0 at 70° C for 30 min. Electrophoresis was performed in 1% agarose gel at 1.5 V/cm for 16 h in TBE buffer supplemented with 0.1 M K-Glu. Gels were stained with 1μg/ml EtBr solution and digitized.

EM experiments were performed with the complexes obtained at various  $R_w$  values in buffer A at 70° C. EM samples were prepared according to Dubochet *et al.* (14): an aliquot (1-2  $\mu$ l) was withdrawn from the reaction mixture and diluted 100-fold in the incubation buffer at room temperature. 5-10  $\mu$ l of this diluted mixture was placed onto a parafilm sheet and covered with an EM grid coated with a thin carbon film (3-4 nm-thick; carbon films were activated by glow-discharge in the presence of pentylamine vapours at a residual pressure of 150  $\mu$ Torr, during 30 sec with the discharge current of 2-3 mA). After 2 - 5 min of adsorption the samples were stained with 2% aqueous uranyl acetate for 10 -15 sec and blotted with filter paper. Where indicated, the samples were further rotary shadowcast at an angle of 7° with tungsten, using the electron gun of an Edwards Auto 306 apparatus. The samples were examined with a Philips CM12 electron microscope in an angular dark-field mode. The negatives were scanned with the Agfa Studio Scan IIsi scanner at 600 dpi. For printing, images were flattened using a high-pass filter with a radius of 250 pixels and adjusted for contrast/brightness using Adobe Photoshop. For the purposes of determining the loop size the smallest *PvuII-PvuII* fragment (474 bp-long) of pPGM1 plasmid DNA was used (15). Length measurements were performed using the NIH Image software modified for Windows by Scion Corporation.

#### Cross-linking experiments

Cross-linking experiments were performed with the complexes obtained after the incubation of pUC19/*Bam*HI DNA, 10  $\mu$ g/ml, with MkaH at  $R_w = 1.5$  in buffer B (0.5 M NaCl, 20 mM Na-Hepes, pH 8.0). Glutaraldehyde was added to a final concentration of 0.1% and incubation was continued for 30 min at room temperature. The reaction was terminated by addition of  $\text{NH}_4\text{Ac}$  to 0.5 M and the mixture was passed through a Sepharose 4B spin-column equilibrated with buffer B. DNase I and  $\text{MgCl}_2$  were added to the eluent to a final concentration of 100  $\mu$ g/ml and 10 mM, respectively, and the mixture was incubated for 30 min at 37° C. The released proteins were separated by SDS/PAGE and transferred onto nitrocellulose membrane as described (16), using a semidry electroblotter with graphite electrodes (DIAM, Russia). MkaH-containing zones were detected using anti-MkaH antiserum and Opti-4CN Detection Kit (Bio-Rad, USA).

#### Analytical gel filtration chromatography

Separations were performed on an analytical liquid chromatography SMART system (Amersham Pharmacia Biotech, Sweden) using a 3.2/30 Superdex 75 column. MkaH was diluted to final concentrations ranging from 0.2  $\mu$ M to 10  $\mu$ M with buffer BC (1 M NaCl, 25 mM Tris-HCl, pH 7.5). 20  $\mu$ l-volume aliquots were applied to the column equilibrated with the BC buffer and run at a flow rate of 50  $\mu$ l/min at room temperature (~23° C). The column was calibrated using ribonuclease A ( $M_r$  13.7 kDa), chymotrypsinogen A ( $M_r$  25 kDa), ovalbumin ( $M_r$  43 kDa), and bovine serum albumin ( $M_r$  67 kDa) as calibration standards. The void volume was determined with Dextran blue ( $M_r$  2 MDa). The partition coefficient,  $K_{av} = (V_e - V_o)/(V_t - V_o)$ , where  $V_e$  is the elution volume,  $V_o$  is the void volume, and  $V_t$  is the gel volume (2.4 ml), was calculated for the samples and standards from triplicate runs.

#### Results

The interaction of MkaH with linear DNA (pUC19/*Bam*HI) in a high-salt buffer (1 M K-Glu) at 70° C led to the formation of stable complexes which could be easily detected by EMSA at room temperature in a running buffer supplemented with 0.1 M K-Glu as a fast migrating band at room temperature (Fig. 1), in accordance with a previous report (17). It is worth noting that due to notable compaction of DNA

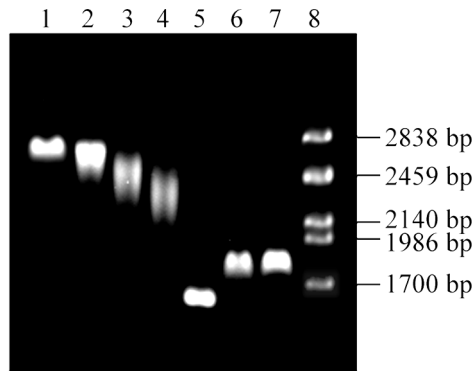


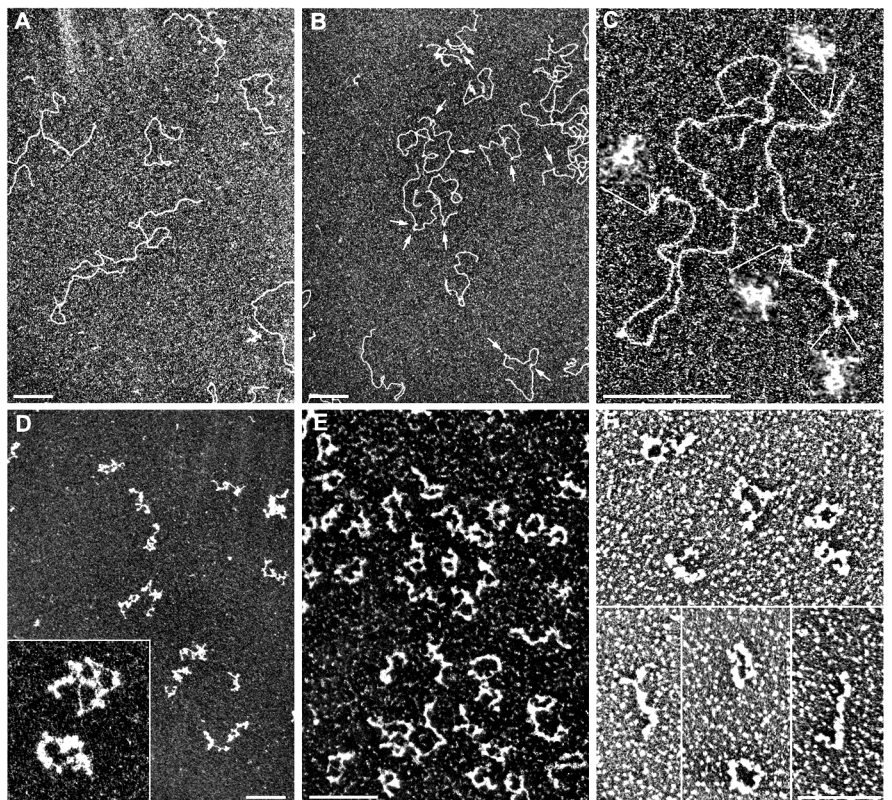
**Figure 1:** Electrophoretic mobility shift assay (EMSA) of MkaH-DNA complexes. *Bam*HI linearized pUC19 DNA (100 ng) was incubated with various concentrations of MkaH in buffer A (see Experimental procedures). Protein-DNA weight ratio in lanes 1 – 7: 0, 0.3, 0.6, 1.5, 3, 9, 15, respectively. Lane 8, *Pst*I digest of bacteriophage  $\lambda$  DNA (lengths in bp are indicated). Electrophoresis was performed in 1% agarose at 1.5 V/cm for 16 h in TBE buffer supplemented with 100 mM K-Glu.

upon binding of MkaH (see below) and low molecular mass of the protein, the electrophoretic mobility of the complex formed with a long DNA fragment was increased relative to that of free DNA in a way similar to that reported for other archaeal histones (17, 18) or the DNA-binding protein from *M. kandleri* (19). While the mobility of the complexes significantly increased with the amount of added protein with the MkaH-DNA weight ratio reaching its maximum at  $R_w \leq 3$  (lanes 2 - 5), a further increase in MkaH concentration resulted in a gradual decrease in complex mobility. At very high protein concentration ( $R_w = 30$ ) complexes disappeared from the gel, probably due to aggregation of protein and DNA that occurred after the transfer of the sample to the conditions required for the electrophoresis (not shown). As expected, EMSA performed in a low-salt buffer (20-30 mM) did not reveal any fast migrating DNA band, most probably due to dissociation of the complexes under these conditions (not shown).

Simultaneously, we examined MkaH-DNA complexes by means of electron microscopy (EM). In order to minimize possible complex dissociation, EM samples were prepared under ionic conditions identical to those used for complex formation, i.e. in the presence of 1M K-Glu. Dilution of the incubation mixture into low-salt buffer (10 mM Tris-HCl, 0.1 mM EDTA) resulted in a fast (1 - 2 min) dissociation of the complexes, leading to images of DNA as protein-free molecules (not shown). At high K-Glu concentration in the mounting buffer (1 M) we detected notable alterations in DNA structure visualized as numerous small loops similar in size with a distinguishable hole in the center (Fig. 2, B, C). The number of loops per single pUC19/*Bam*HI DNA molecule gradually increased with the amount of added protein from 2 - 3 ( $R_w = 0.3$ ) to about 13 ( $R_w = 1.5$ ), corresponding to a mean loop-loop distance of  $\sim 700$  bp and  $\sim 200$  bp, respectively.

At  $R_w = 3$ , for which the highest mobility of the complex was observed (Fig. 1, lane 5), individual loops were still visible, though a major fraction appeared juxtaposed, often overlapping, leading to a significant apparent thickening of DNA molecules (Fig. 2, D). A further increase in protein concentration ( $R_w = 9$ ) led to more condensed structures of variable length and thickness, in which individual loops could hardly be discerned (Fig. 2, E, F). The condensed structures were mostly linear,

**Figure 2:** Electron microscopy of the complexes formed by MkaH with pUC19/*Bam*HI DNA. Complexes were obtained after the incubation in buffer A at  $R_w = 0$  (A), 0.3 (B, C), 3 (D), and 9 (E, F). (C, D) insets, enlarged views of individual loops and complexes. Images were taken from samples stained with uranyl acetate (A-E) or tungsten shadowcast (F). Arrows indicate DNA loops (B). Scale bars represent 200 nm.



although some exhibited a ring-like appearance, possibly stabilized via interaction of proteins bound at DNA termini. Essentially, the apparent contour length of these complexes was notably smaller than that of naked DNA (~3-4 times).

In order to determine the DNA length involved in loop formation, we used a 474 bp-long DNA fragment and measured the contour length of loop-free segments as a function of the number of loops (Fig. 3). There was a linear reduction in DNA contour length and a decrease in the number of loops, corresponding to  $71 \pm 7$  bp of DNA duplex constrained within the loops.

To evaluate the stoichiometry of MkaH-DNA complexes, the complexes were cross-linked by glutaraldehyde and purified from unbound protein by passage through a Sepharose 4B spin-column. Prior to this, we determined the dominant oligomerization form of the protein in solution in the absence of DNA. By using Western immunoblotting analysis, we determined the presence of one major product of ~34 kDa (Fig. 4A, lane 2) corresponding to the MkaH dimer and in agreement with gel filtration chromatography (see below). In the presence of DNA, residual proteins released from the complexes were of ~17 and ~34 kDa (Fig. 4A, lane 3), corresponding to the MkaH monomer (17,004 Da) and dimer (34,008 Da), respectively. Due to random interactions of glutaraldehyde with accessible residues of amino acids, thus partially preventing formation of stable bridges between residues of amino acids from adjacent protein monomers, the presence of MkaH monomers was to be expected; as a result, chemically modified but unlinked proteins were run as monomers through SDS/PAGE gel (see Materials and Methods).

The MkaH self-association properties were further characterized by analytical gel filtration chromatography. We found that MkaH loaded to the column at a concentration within the range from 0.5  $\mu$ M to 10  $\mu$ M eluted consistently as a single peak. The calibration plot (Fig. 4B) shows a dependence of the mean partition coefficient  $K_{av}$  of standard proteins (calculated from triplicate run data) on the logarithm of their molecular weight. The partition coefficient calculated for MkaH at all studied concentrations coincided with an apparent molecular weight of ~36 kDa, providing evidence of the self-association, i.e. dimerization, behavior of the protein in solution.

## Discussion

In this study, we characterized the DNA binding properties of MkaH, an unusual "oversized" histone from hyperthermophile *M. kandleri*. It has been recently shown that in the presence of potassium glutamate ( $\geq 150$  mM) and elevated temperatures ( $\geq 70^\circ$ ) the binding of MkaH to covalently closed circular substrates produced negative supercoils in a DNA topology assay (17). However, the mechanisms of MkaH interaction with DNA leading to negative supercoiling were unclear. Our data show that MkaH upon DNA binding constrains  $71 \pm 7$  bp of DNA duplex into loops, which are very stable in the presence K-Glu and room temperature as well. We suppose that formation of these loops (left-handed in accordance with (17)) is the main mechanism of MkaH interaction with DNA. The loops can be separated by long stretches of free DNA or are juxtaposed depending on the protein-DNA ratio, ultimately leading to short, thick condensed aggregates with scarcely discernible individual loops. We speculate that the thickest segments of such aggregates arise from the stacking of adjacent loops stabilized by protein-protein interactions between individually bound proteins. Some aggregates had a ring-like structure that could have resulted from the interactions of MkaH dimers on both termini of linear DNA. It should be noted that EM analysis of the complexes formed at  $R_w < 3$  did not reveal classical beads on a string, but rather isometric loops with a distinguishable hole in the center. We attribute the lack of a histone-like appearance to selective staining of the DNA with the uranyl acetate. A similar phenomenon has been observed for eukaryal nucleosomes (20), eukaryal tetrasomes (9) and archaeal histons (10). The length of the loop-constrained DNA

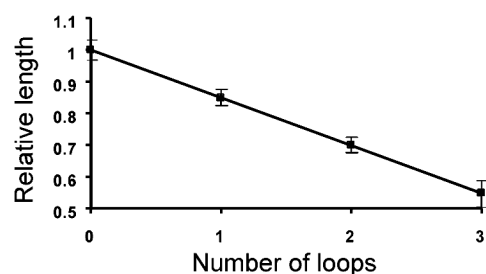


**Figure 3:** DNA condensation by interaction with MkaH. The length of loop-free segments of a 474 bp-long DNA fragment was measured, normalized by the entire length of the fragment, and plotted against the number of individual loops formed with the fragment. Number of measured DNA fragments: 0 loops, 16; 1 loop, 37; 2 loops, 19; 3 loops, 14. The straight line (least square fit) corresponds to a loop size of  $71 \pm 7$  bp (S. D.).

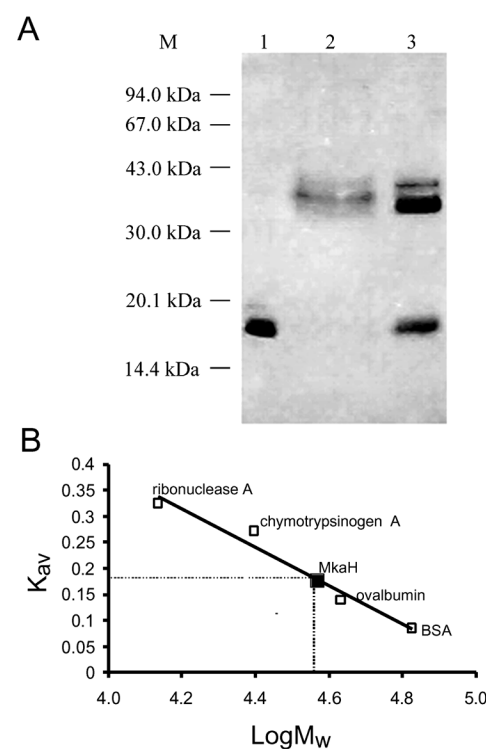


**Figure 4:** Oligomerization properties of MkaH protein. **A.** The panel represents an electrophorogram of intact MkaH in the absence of DNA previous to (lane 1) and after chemical fixation with 0.1% glutaraldehyde (lane 2). Lane 3, released products from the cross-linked with 0.1% glutaraldehyde MkaH-DNA complexes; the complexes were obtained at  $R_w = 1.5$  and purified from DNA (see Experimental procedures). Proteins were detected by Western immunoblotting. M, molecular weight markers. **B.** Gel-filtration of MkaH. Calibration plot relating the observed partition coefficients ( $K_{av}$ ) to the log of molecular weights ( $\text{Log}M_w$ ) of standard proteins is shown. The line representing a least square regression was used to determine the apparent molecular weight of MkaH.

duplex corresponded to  $71 \pm 7$  bp, a length that is compatible with that of the major DNA fragment protected by MkaH from MNase digestion (17).

How the loops are stabilized by bound MkaH is as yet unclear. A plausible explanation is that the dimer of MkaH, the dominant stable form of the protein in solution and in the complex, brings two distal DNA duplexes into close proximity (through DNA bending). However, we consider this mechanism unlikely in view of the length of the loop-constrained duplex ( $71 \pm 7$  bp) and the small size of the protein ( $\sim 34$  kDa for a dimer). Moreover, this mechanism would require significant structural rearrangement of the protein upon DNA circularization. Another conceivable model is that DNA is wrapped around a dimer of MkaH forming left-handed superhelical DNA loop in a way(s) reviewed in (21, 22). Still, it is yet unclear how many dimers are needed for such DNA bending and looping. According to cross-linking experiments, the dimer is the dominant form of the protein in the complex at least for low and moderate values of  $R_w$  ( $< 3$ ). No higher order protein aggregates were detected. However, it cannot be ruled out that a number of non-interacting MkaH dimers contribute to the formation of loop-constrained DNA.

In general, our data correspond to the current model of the archaeal nucleosome-like particle as a structural homologue of the eukaryal tetrasome. It has been shown previously that the homodimer of HMfB (histone from *Methanothermobacter feravidus*) facilitates circularization of 83 bp-long linear DNA fragment by DNA ligase, presumably due to DNA wrapping (12), that chemically fixed *in vivo* nucleosome-like particles from *Methanobacterium thermoautotrophicum* protect from MNase digestion  $\sim 60$  bp DNA (23), and that the HMf-DNA complex contains a histone tetramer rather than an octamer (12, 23).

However, some DNA binding properties of MkaH seem to be atypical. As shown by chemical cross-linking and gel filtration chromatography, MkaH in solution exists as a stable dimer (tetrameric histone-fold assembly), like the eukaryal  $(H3-H4)_2$  (7), but unlike other archaeal proteins (24). We hypothesize that formation of the MkaH-DNA complex occurs in a manner similar to that of the tetrasome, i.e., by direct wrapping of DNA around the preformed protein core. In contrast, the HMf-type nucleosome is assembled in a stepwise fashion, with the intermediate structure imaged as a sharp DNA kink and interpreted as a complex of DNA with a single histone dimer (10).

Our finding is in agreement with recent structural data obtained for both MkaH (13) and HMf-like histones (11, 25, 26). Based on X-ray and NMR analysis, the HMf dimer is not prone to further oligomerization in crystal or in solution, whereas MkaH self-associates in the crystal (*via* the characteristic four-helix-bundle motif) resulting in a structure aligned well with the  $(H3-H4)_2$  tetramer (root mean square deviation  $\sim 2.0 \text{ \AA}$ ). It is worth noting that MkaH also lacks a hydrogen-bonded proline tetrad, the novel structural motif characteristic of all other archaeal histones characterized to date but absent in the eukaryal proteins (27). Interestingly, the HpyA histone isolated from *Halobacterium* sp. NRC-1, which is akin to MkaH through the presence of histone-fold domain repeat, does contain a proline tetrad motif, as can be predicted from the amino acid sequence.

The crystal structure of the MkaH dimer differs from that of  $(H3-H4)_2$  in the nucleosome by the following feature. While two H3-H4 dimers are drawn together exclusively by a four-helix-bundle,  $MkaH_2$  has an additional stabilizing contact formed by C-terminal residues of  $\alpha 3C$  helices. It has been suggested that arm closure of the V-shaped  $MkaH_2$  structure prevents formation of four-helix-bundle interfaces with other dimers (13). Nevertheless, MkaH dimer may possibly oligomerize further under certain conditions, for example, in a DNA bound state and at high  $R_w$  values, yielding tetramers (or pseudo-octamers of histone-fold

domain!) and higher order multimers. It is unclear whether the observed compact nucleoprotein complexes are related to the *in vivo* function of MkaH. To our knowledge, the observation of a 17-20 nm-width rugged thick fiber in the archaeon *Halobacterium salinarium* is the only indication of the existence of higher order archaeal chromatin structures (28).

Further experiments are required to determine which functional features of MkaH-containing archaeal nucleosome are caused by the interaction of the protein's  $\alpha 3C$  helices. The majority of archaeal nucleosomes, with the exception of those formed by MkaH, display a change in DNA topology of the constrained DNA upon lowering the salt concentration (17). This property has been related to the tetrasome "flipping", a change in the handedness of DNA and proteinaceous superhelices induced by DNA torsional constraint and apparently mediated by deformation and mutual reorientation of H3-H4 dimers (29). If interaction of the C-terminal helices persists in the MkaH-DNA complex, "flipping" would be hindered even under the pressure of high DNA torsional stress.

### Acknowledgements

The authors gratefully acknowledge Dr. Galina Belova for her help with protein purification and Dr. Vinod Subramaniam for critically reading the manuscript. This work was supported by a FEBS short-term fellowship (to N. P.) and by grants from HHMI, RFBR and NIH (to A. S.).

### References and Footnotes

1. M. Kurr, R. Huber, H. König, H. W. Jannasch, H. Fricke, A. Trincon, J. K. Kristjansson and K. O. Stetter, *Arch. Microbiol.* 156, 239-247 (1991).
2. A. I. Slesarev, K. O. Stetter, J. A. Lake, M. Gellert, R. Krahl and S. A. Kozyavkin, *Nature* 364, 735-737 (1993).
3. A. I. Slesarev, J. A. Lake, K. O. Stetter, M. Gellert and S. A. Kozyavkin, *J. Biol. Chem.* 269, 3295-3303 (1994).
4. S. Burggraf, K. O. Stetter, P. Rouviere and C. R. Woese, *Syst. Appl. Microbiol.* 14, 346-351 (1991).
5. A. I. Slesarev, G. I. Belova, S. A. Kozyavkin and J. A. Lake, *Nucleic Acids Res.* 26, 427-430 (1998).
6. K. Luger, A. W. Mader, R. K. Richmond, D. F. Sargent and T. J. Richmond, *Nature* 389, 251-260 (1997).
7. T. H. Eickbush and E. N. Moudrianakis, *Biochemistry* 17, 4955-4964 (1978).
8. F. Dong and K. E. van Holde, *Proc. Natl. Acad. Sci. USA* 88, 10596-10600 (1991).
9. A. Hamiche, V. Carot, M. Alilat, F. De Lucia, M. F. O'Donohue, B. Revet and A. Prunell, *Proc. Natl. Acad. Sci. USA* 93, 7588-7593 (1996).
10. K. Sandman, J. A. Krzycki, B. Dobrinski, R. Lurz and J. N. Reeve, *Proc. Natl. Acad. Sci. USA* 87, 5788-5791 (1990).
11. M. R. Starich, K. Sandman, J. N. Reeve and M. F. Summers, *J. Mol. Biol.* 255, 187-203 (1996).
12. K. A. Bailey, C. S. Chow and J. N. Reeve, *Nucleic Acids Res.* 27, 532-536 (1999).
13. R. L. Fahrner, D. Cascio, J. A. Lake and A. Slesarev, *Protein Sci.* 10, 2002-2007 (2001).
14. J. Dubochet, M. Ducommun, M. Zollinger and E. Kellenberger, *J. Ultrastruct. Res.* 35, 147-167 (1971).
15. D. I. Cherny, G. Striker, V. Subramaniam, S. D. Jett, E. Palecek and T. M. Jovin, *J. Mol. Biol.* 294, 1015-1026 (1999).
16. N. L. Anderson, S. L. Nance, T. W. Pearson and N. G. Anderson, *Electrophoresis* 3, 135-142 (1982).
17. D. Musgrave, P. Forterre and A. Slesarev, *Mol. Microbiol.* 35, 341-349 (2000).
18. K. Sandman, R. A. Grayling, B. Dobrinski, R. Lurz and J. N. Reeve, *Proc. Natl. Acad. Sci. USA* 91, 12624-12628 (1994).
19. N. A. Pavlov, D. I. Cherny, I. V. Nazimov, A. I. Slesarev and V. Subramaniam, *Nucleic Acids Res.* 30, 685-694 (2002).
20. G. Moyne, R. Freeman, S. Saragosti and M. Yaniv, *J. Mol. Biol.* 149, 735-744 (1981).
21. A. Travers and H. Drew, *Biopolymers* 44, 423-433 (1997).
22. A. Travers and G. Muskhelishvili, *J. Mol. Biol.* 279, 1027-1043 (1998).
23. S. L. Pereira, R. A. Grayling, R. Lurz and J. N. Reeve, *Proc. Natl. Acad. Sci. USA* 94, 12633-12637 (1997).
24. R. A. Grayling, K. Sandman and J. N. Reeve, *Adv. Protein Chem.* 48, 437-467 (1996).
25. K. Decanniere, A. M. Babu, K. Sandman, J. N. Reeve and U. Heinemann, *J. Mol. Biol.* 303, 35-47 (2000).

26. W. Zhu, K. Sandman, G. E. Lee, J. N. Reeve and M. F. Summers, *Biochemistry* 37, 10573-10580 (1998).
27. K. Sandman, D. Soares and J. N. Reeve, *Biochimie* 83, 277-281 (2001).
28. S. Takayanagi, S. Morimura, H. Kusaoka, Y. Yokoyama, K. Kano and M. Shioda, *J. Bacteriol.* 174, 7207-7216 (1992).
29. M. Alilat, A. Sivolob, B. Revet and A. Prunell, *J. Mol. Biol.* 291, 815-841 (1999).

*Date Received: July 17, 2002*

**Communicated by the Editor Ramaswamy H Sarma**